Carbohydrate Polymers 79 (2010) 547–554

Contents lists available at ScienceDirect

Carbohydrate Polymers

journal homepage: www.elsevier.com/locate/carbpol

Optimization of mechanical properties of thermoplastic starch/clay nanocomposites

Kazem Majdzadeh-Ardakani, Amir H. Navarchian *, Farhad Sadeghi

Department of Chemical Engineering, Faculty of Engineering, University of Isfahan, P.O. Box 81746-73441, Isfahan, Iran

ARTICLE INFO

Article history:
Received 25 June 2009
Received in revised form 12 August 2009
Accepted 7 September 2009
Available online 11 September 2009

Keywords:
Starch
Clay
Nanocomposite
Young's modulus
Morphology

ABSTRACT

Starch/clay nanocomposites were prepared via solution casting method and the effects of starch source, clay cation, glycerol content, and mixing mode on clay intercalation and Young's modulus of nanocomposites were investigated using a Taguchi experimental design approach. The clay intercalation was examined by X-ray diffraction (XRD) patterns. Nanocomposites prepared with montmorillonite (MMT) modified with citric acid demonstrated the highest Young's modulus compared to pristine MMT and organoclay. A combined mechanical and ultrasonic mixing mode led to an extensive dispersion of silicate layers and thus the highest Young modulus in nanocomposites. The effect of clay content on tensile properties was also investigated. It was observed that the maximum stress strength would be attained for nanocomposite films with 6% (by weight) of clay loading. The chemical structure and morphology of the optimum sample was probed by FT-IR spectroscopy and transmission electron microscopy (TEM).

1. Introduction

In order to solve problems generated by plastic waste many efforts have been done to obtain an environmental friendly material. Most of the researches are focused on substitute oil-based plastics by biodegradable materials with similar properties (Cyras, Manfredi, Ton-That, & Vazquez, 2008). Starch is known to be completely biodegradable in soil and water, and due to its cheap sources is one of the best candidates for replacing current synthetic plastics including packaging materials (Park, Lee, Park, Cho, & Ha, 2003). The thermoplastic starch (TPS) is obtained after disruption and plasticization of starch macromolecules by heating in presence of water and plasticizers such as glycerol. The products made from TPS are however water sensitive and would present inferior mechanical and physical properties. The mechanical weaknesses of these materials for packaging application can be usually improved by incorporation of a synthetic polymer or an inorganic reinforcing material including montmorillonite (MMT) (Curvelo, Carvalho, & Agnelli, 2001; Sorrentino, Gorrasi, & Vittoria, 2007; Wilhelm, Sierakowski, Souza, & Wypych, 2003). Application of MMT is of great interest nowadays due to its natural source, high modulus of clay platelets (Ray & Bousmina, 2005), and low content necessary to attain the desired mechanical properties. These layered materials there exist in the form of the aggregates bonded with physical forces, so that they can be exfoliated even to single nanolayers and results in TPS/MMT nanocomposite (Ray & Bousmina, 2005). The silicate layers can also play the role of barrier and therefore inhibits the diffusion of water and oxygen through the packaging film (Cyras et al., 2008; Ray & Bousmina, 2005).

Crystal lattice of MMT consists of two-dimensional layers in which a central octahedral sheet of alumina or magnesia is fused to two external silica tetrahedrons (Hasebawa, Kawasumi, Kato, Usuki, & Okada, 1998; Kampeerapappun, Aht-ong, Pentrakoon, & Srikulkit, 2007; Ray & Bousmina, 2005). Due to presence of sodium cations between the interlayer spaces (galleries), the natural MMT is hydrophilic and is miscible with hydrophilic polymers including starch (Park et al., 2003; Ray & Bousmina, 2005).

The various processing methods used to prepare starch nanocomposites cause different filler distribution and exfoliation of the clay layers (Dean, Yu, & Wu, 2007; Park et al., 2003). Many authors have investigated the effects of extrusion variables on melt intercalation of starch/clay nanocomposites (Chen & Evans, 2005; Chiou, Yee, Glenn, & Orts, 2005; Dean et al., 2007). The effect of clay content on physical and mechanical properties of these nanocomposites has also been studied (Chen & Evans, 2005; Chiou et al., 2005; Cyras et al., 2008; Park et al., 2003; Wilhelm et al., 2003). The ultimate properties could be influenced by the factors including the type of cation or modifier in clay (Chen & Evans, 2005; Chiou et al., 2005; Park et al., 2003), the method of clay dispersion (Dean et al., 2007), the glycerol content (Chiou et al., 2007; Pandey & Singh, 2005; Yu, Wang, Wu, & Zhu, 2008) and the starch resources (Mondragon, Mancilla, & Rodriguez-Gonzalez, 2008). The effects of these parameters have been individually studied in the literature on one or a couple of product properties, while the other factors were kept unchanged.

* Corresponding author. Tel.: +98 311 793 4014; fax: +98 311 793 4031.
E-mail addresses: Navarchian@eng.ui.ac.ir, anavarchian@yahoo.com (A.H. Navarchian).

0144-8617/$ - see front matter © 2009 Elsevier Ltd. All rights reserved.
doi:10.1016/j.carbpol.2009.09.001

The Taguchi experimental design method is a statistical approach that reduces the number of experiments necessary for investigating the effects of various parameters on the product quality and/or quantity. This method also screens the significant factors affecting the response from those with less significance, and gives the optimum condition to attain the most desirable performance. Although there are, many papers recently published on the starch/clay nanocomposite field, there is no report available regarding application of experimental design for comparative analysis of the effects of material and mixing parameters on the physical and mechanical properties of starch/clay nanocomposites. Moreover, little attention has been paid on solution casting method for preparation of these nanocomposites. In this study, the influences of starch source (A), clay cation (B), glycerol content (C) and mixing mode (D) on the modulus of starch/clay nanocomposites prepared via solution method have been statistically investigated by using Taguchi experimental design approach. The relationship between the silicate layers spacing distance and the modulus improvement have been studied. Finally, the optimum conditions to attain the maximum Young's modulus have been obtained, and the effect of clay content has been studied on the physical and mechanical properties of nanocomposites at optimal conditions of starch source, clay cation, glycerol content and mixing mode.

2. Experimental

2.1. Materials

Three different types of starch included corn (Glucozan Co., Ghazvin, Iran), wheat and potato (Merck KGaA, Darmstadt, Germany) with different amylose and amylopectin contents were used (the amylose content of corn, wheat and potato starches was 28, 30 and 20 wt.%, respectively). Sulfuric acid (98%), citric acid ($C_6H_8O_7$) with 1.665 g/cm^3 density and glycerol (about 87% purity) were obtained from Merck KGaA, Darmstadt, Germany. Cloisite®Na^+ (MMT) as untreated montmorillonite and Cloisite®30B (30B–MMT) with ammonium ions (90 mequiv./100 g clay) were purchased from Southern Clay Products (USA) and were used as received. The ammonium ion was methyl-tallow-bis-2-hydroxyethyl (MT 2EtOH) with the chemical formula of $N^+(C_2H_4OH)_2(CH_3)T$, where T represents an alkyl group of approximately 65% $C_{18}H_{37}$, 30% $C_{16}H_{33}$, and 5% $C_{14}H_{29}$. The other modified clay (CMMT) was prepared in our laboratory by cation exchange of Na^+ in MMT with citric acid, as discussed later.

2.2. Design of experiments

The simple approach in research process involves changing one parameter at a time. This approach requires numerous experimental runs to fully explore the entire parameter space. The experimental design approach such as Taguchi method can be introduced as an effective technique to reduce the number of experiments while retaining quality of data collection.

The first important step in design of the experiments is the proper selection of factors and their levels. In this study, four main factors: starch source, clay cation, glycerol content and mixing mode were considered in three levels (Table 1). The factors and their levels have been selected according to a literature review on previous publications (Chen & Evans, 2005; Chiou et al., 2007; Dean et al., 2007; Pandey & Singh, 2005; Park et al., 2003; Yu et al., 2008), the practical aspects, and some screening experiments. For Taguchi-design of experiments with four factors and three levels for each factor, a standard L_9 orthogonal array was employed as shown in Table 2 (Roy, 2001). Each row of the matrix represents one run at specified condition. In order to avoid the systematic bias, the sequence in which these runs were carried out was randomized (Park, 1996; Roy, 2001).

Table 1
Selected factors and their respective levels.

Factors	Symbol	Level 1	Level 2	Level 3
Starch source	A	Corn	Potato	Wheat
Clay cation	B	30B–MMT	MMT	CMMT
Glycerol content (wt.%)	C	10	20	30
Mixing mode	D	Mechanical	Combined	Ultrasonic

Table 2
Taguchi L_9 orthogonal array of designed experiments based on the coded levels.

Trial	Factors			
	A	B	C	D
1	Corn	30B–MMT	10	Mechanical
2	Corn	MMT	20	Combined
3	Corn	CMMT	30	Ultrasonic
4	Potato	30B–MMT	20	Ultrasonic
5	Potato	MMT	30	Mechanical
6	Potato	CMMT	10	Combined
7	Wheat	30B–MMT	30	Combined
8	Wheat	MMT	10	Ultrasonic
9	Wheat	CMMT	20	Mechanical

2.3. Preparation of modified MMT with citric acid

About 1.68 g of citric acid (8.75 mmol) and 0.8 ml of sulfuric acid (98%) were added subsequently to 230 ml water at 80 °C in a 500 cc beaker. This solution was gradually added to a clay suspension containing 5 g MMT in 100 ml water. The mixture was stirred at 80 °C for 3 h, and then cooled to room temperature. It was then filtered, and the cake was washed with distilled water and centrifuged for 30 min. The modified clays were dried at 60 °C for 24 h, and then ground into a fine powder. The citric acid-activated montmorillonite (CMMT) was obtained after screening (Huang, Yu, & Ma, 2006).

2.4. Preparation of thermoplastic starch/clay nanocomposite films

Starch/clay nanocomposite films were prepared via solution casting technique. About 4 g of specified type of starch was first dispersed in 60 ml distilled water with 10, 20 or 30 wt.% of glycerol according to the corresponding run of experiments. The suspension was then heated to 70 °C for 1 h under vigorous stirring. Specified amount of dried clay (5 wt.% relative to dry starch) was dispersed at room temperature in 40 ml distilled water by one of the following mixing modes:

- Mechanical mixing with a 5-cm conventional impeller at1600 rpm for 1 h, using a RW 20.n mixer (IKA, USA) in a 100 ml beaker.
- Sonication mixing for 1 h was performed on a HD 2200 ultrasonic homogenizer (Bandelin, Germany) with the high-frequency power at a frequency of 20 kHz and 6 mm probe diameter.
- Mechanical mixing for 30 min was followed by sonication for 30 min (denoted as "combined").

The clay suspension was added to the aqueous dispersion of starch and the mixing was continued for 10 min at 70 °C. The mixture was degassed under vacuum and then was heated to boiling temperature for 30 min with continuous stirring to gelatinize the starch granules. After mixing, suspensions were degassed under

vacuum again. The nanocomposite films were obtained by pouring the hot suspension into rectangular Teflon molds and dried in oven at 45 °C for 24 h. The thickness of the films, measured by micrometer, was 0.2 ± 0.02 mm.

In the second section of experiments the starch nanocomposite films were prepared with different loadings of clay (0, 3, 4, 5, 6, 7, 10 and 15 wt.%) where the other factors were kept at their optimum levels determined by the first set of experiments.

2.5. Characterization of nanocomposite films

X-ray diffraction (XRD) analysis was carried out on a Bruker D8 Advance X-ray diffractometer (Bruker, Germany) using CuKα radiation (40 kV, 40 mA and $\lambda = 0.154$ nm). Samples were scanned at 1°/min in the range of $2\theta = 2$–10°. The basal spacing of the silicate layer, $d_{(0\,0\,1)}$, was calculated using the Bragg's equation ($n\lambda = 2d \sin\theta$), where θ is the diffraction angle and λ is the wavelength.

Tensile tests were performed according to the ASTM D882-02 by using SMT-5 tester (Santam, Iran). The crosshead speed was 10 mm/min. Rectangular specimens were conditioned at 50 ± 5% RH and 23 ± 2 °C for one week before testing.

Furrier Transformed Infrared (FT-IR) spectra of nanocomposite films were measured by Nicolet 400D Impact spectrometer (Nicolet Instrument Corporation, USA) in the range of 450–4000 cm^{-1} and with a resolution of 16 cm^{-1}.

Transmission electron microscope (TEM) was employed for microscopic observation of internal morphology of nanocomposite films. A CM10 microscope model (Philips, Germany), operating at an accelerating voltage of 100 kV was used.

3. Results and discussion

3.1. XRD data of clays and nanocomposites

Wide angle X-ray diffraction (WAXD) is a common technique used in examining the intercalation and/or exfoliation of silicate layers. The XRD patterns of natural MMT, CMMT and 30B–MMT have been shown in Fig. 1. A characteristic diffraction peak is appeared at $2\theta = 7.96°$ for MMT, at 5.98° for CMMT and at 5.01° for 30B–MMT corresponding to gallery spacing of 1.11, 1.48 and 1.76 nm, respectively.

In the case of 30B–MMT and CMMT, the organic cation (ammonium ion) and citric acid molecule penetrate into the interlayer space of clay and replace the sodium cations. That would result in enlarging of the gallery spacing and hence a shift in the peak position to a lower angle in the XRD pattern. The gallery spacing distance is proportional to the size of cation or molecule between the layers. Thus the sodium cation with the atomic radius of 1.02 Å (Yaws, 1999) and the ammonium ion with long chain alkyl groups that results in a large radius of gyration, resulted in the smallest and the greatest interlayer spacing in MMT and 30B–MMT, respectively.

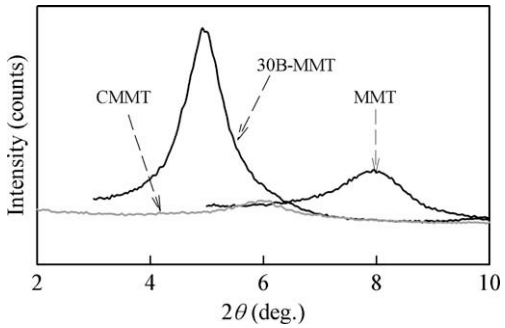

Fig. 1. XRD patterns of MMT, CMMT and 30B–MMT.

The XRD data for nanocomposite films prepared at different conditions are presented in Table 3. The difference between *d*-spacing of clays in nanocomposite films (d_{nc}) and that of corresponding pristine clays (d_0) is reported as Δd ($\Delta d = d_{nc} - d_0$) in this table. The data show that the largest Δd corresponds to the CMMT-filled samples. The citric acid molecules play a roll of bridge between clay surface and starch molecules through hydrogen bonding. This leads to higher efficiency of intercalation process and thus a large interlayer spacing of silicate layers in corresponding nanocomposites.

3.2. Relation between Young's modulus and gallery spacing

The results of tensile properties measurements for the samples have been listed in Table 3. The higher Young's modulus (*E*) is observed for the samples filled by CMMT. This is due to higher degree of dispersion of silicate layers in these nanocomposites as confirmed also by XRD data.

Correlation between *E* and Δd is shown in Fig. 2. It is observed that the Young's modulus increases almost linearly with the gallery spacing, regardless of the experimental conditions during sample preparation. The greater gallery spacing is a representative of more starch molecules diffuse into the space between the silicate layers and thus higher interfacial interactions that lead to more intensive reinforcing effects.

3.3. Analysis of variance for Δd and tensile strength

The analysis of variance (ANOVA) is a powerful technique in Taguchi method that explores the percent contribution of factors affecting the response. The strategy of ANOVA is to extract the variations that each factor cause relative to the total variation observed in the results (Montgomery, 1997; Roy, 2001). The statistical analysis of the results was carried out using Qualitek-4 (Nutek Inc.) software. Table 4 shows the ANOVA statistical terms for Young's modulus of nanocomposites.

The *F*-ratio in ANOVA table is a reliable criterion for ranking the factors with respect to their influence. A higher value of the calculated *F*-ratio for a factor means a greater influence of that factor on the experiment outcome. Moreover, if the percent contribution of a factor would be equal to or less than 10% of that of the most affecting factor, this factor can be pooled with error terms (Roy, 2001). It is clear from Table 4 that the most important contributors to the variability of the results are clay cation (B) and clay mixing mode (D). The starch source (A) however has a less pronounced effect in ANOVA table, and therefore it is pooled with error term, with a 90% confidence level. The other/error term, in the last row of ANOVA table, contains thus the information about three sources of variability of the results including uncontrollable factors, factors that are not considered in the experiments, and the experimental error (Roy, 2001). It should be emphasized that the interpretation of ANOVA table is valid just in the range of considered levels for the factors. That's why the determination of levels is of great importance in any experimental design approach.

In the following sections the effects of various factors on gallery spacing distance and thus on Young's modulus are comprehensively investigated.

3.4. Effects of factors on gallery spacing and tensile properties

The trends in which *E* and Δd are influenced when the factors are varied on their levels are shown on main-effect plots (Fig. 3). Each point on these plots represents the average of three experimental data.

Table 3
XRD data and mechanical properties of samples.

XRD data			Mechanical properties		
Trial	2θ of the peak (°)	Δd (nm)	Tensile stress (MPa)	Young's modulus (MPa)	Elongation at break (%)
1	4.72	0.11	2.0	7.5	73.3
2	5.00	0.66	9.2	131.5	25.2
3	4.52	0.47	5.0	84.1	62.8
4	4.30	0.29	2.5	41.7	76.6
5	6.59	0.23	2.4	19.1	84.8
6	3.80	0.84	28.1	187.5	57.3
7	4.50	0.20	2.9	17.8	68.3
8	6.26	0.30	3.8	54.2	91.9
9	4.20	0.62	3.1	112.4	29.4

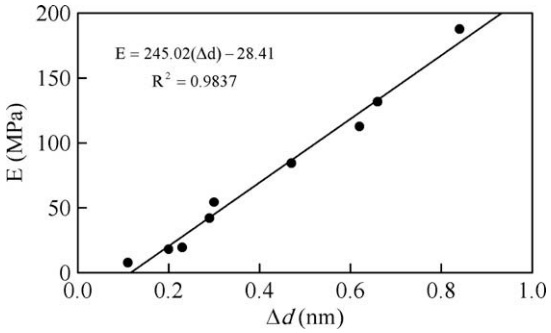

Fig. 2. Correlation between Young's modulus and gallery spacing (Δd) of nanocomposites with 5 wt.% of various clays.

3.4.1. Effect of clay cation

The effect of clay cation (or modifier) on Δd and Young's modulus of starch/clay samples is observed in Fig. 3a. The first level of clay cation (30B–MMT) results in lower Young's modulus and gallery spacing (Δd) compared to that of MMT and CMMT. This is expected as there is no significant clay–polymer interaction between 30B–MMT (with hydrophobic ion) and starch (with hydrophilic character). In starch/MMT and starch/CMMT nanocomposites, the sodium cation or acid citric molecule provide interfacial interactions with starch matrix, and therefore improve the exfoliation of the layered host into its nanoscale elements (Dean et al., 2007). This in turn improves the mechanical properties of the sample (Huang et al., 2006). The Young's modulus for nanocomposites filled by CMMT in this work is much higher than values reported by other authors for biodegradable films (Avella et al., 2005; Tang, 2008). In fact the H-bonding interaction between hydrated sodium cation in MMT and the OH groups of citric acid modifier in CMMT, with the free OH groups residing in the starch chains could facilitate the dispersion of clay platelets throughout the starch matrix. The intensive interaction between acid citric and starch, as well as the wide gallery spacing of CMMT that facilitate the penetration of starch chains, is probably responsible for the highest Young's modulus of TPS/CMMT nanocomposites.

The maximum value of gallery expansion (Δd = 0.84 nm) obtained for TPS/CMMT nanocomposites in this work is much higher than those obtained by other authors for TPS/clay nanocomposites prepared via solution casting technique (Cyras et al., 2008; Kampeerapappun et al., 2007; Mondragon et al., 2008; Wilhelm et al., 2003). The second one is 0.52 nm that is reported by Cyras et al. (2008) for a similar system.

3.4.2. Effect of mixing mode

It is implied from the data in ANOVA table (Table 4), that after the clay cation, the mixing mode (D) is ranked the second in affecting the factors of Δd and E. As observed in Fig. 3b, Δd and E represent the highest improvement when a combination of ultrasonic and mechanical mixing is applied for dispersing the silicate layers throughout the water. Neither the mechanical mixing nor sonication alone has a remarkable influence on the dispersion degree of silicate layers (and therefore tensile properties of nanocomposites).

The individual particles of clays in water are held together by van der Waals forces. The shear forces due to mixing modes have to overcome these forces as well as the liquid surface tension in order to disperse the particles into the liquid media. In addition, a proper distribution of individual silicate layers is necessary in order to attain a homogeneous accumulation of nano-fillers throughout the matrix (Ray & Bousmina, 2005).

A comprehensive discussion on mixing mechanisms can interpret well the effect of mixing modes in current work. Generally, there are two mechanisms of mixing solid particulates in a viscous liquid. Dispersive mixing is defined as the breakup of agglomerates to the desired ultimate grain size of the solid particulates (individual silicate layers). On the other hand, distributive mixing means providing a spatial uniformity of all the components in system. The ultrasonic device just provides a dispersive mixing, while the mechanical mixer can mainly contribute to distribution of domains in the matrix (Paul, Atiemo-Obeng, & Kresta 2004). Therefore, a combination of both mixing methods can lead to an appropriate uniform mixing that is vital in polymer/clay nanocomposites.

The breaking of agglomerates and dispersion by sonication are the results of ultrasonic cavitation. When exposing liquids to ultrasound, the sound waves propagate into the liquid and result in

Table 4
ANOVA table for Young's modulus (E).

Factors	DOF[a]	Sum of squares	Variance	F-ratio	Pure sum	Percent
Starch source	2	690.45	POOLED (CL = 90%)			0.000
Clay cation	2	16843.40	8421.70	24.39	16152.94	54.22
Glycerol content (%)	2	4983.93	2491.96	7.21	4293.48	14.41
Mixing mode	2	7269.56	3634.78	10.52	6579.10	22.08
Other/error	2	690.46	345.23	–	–	9.27
Total	8	29787.36				100.00%

[a] Degree of freedom.

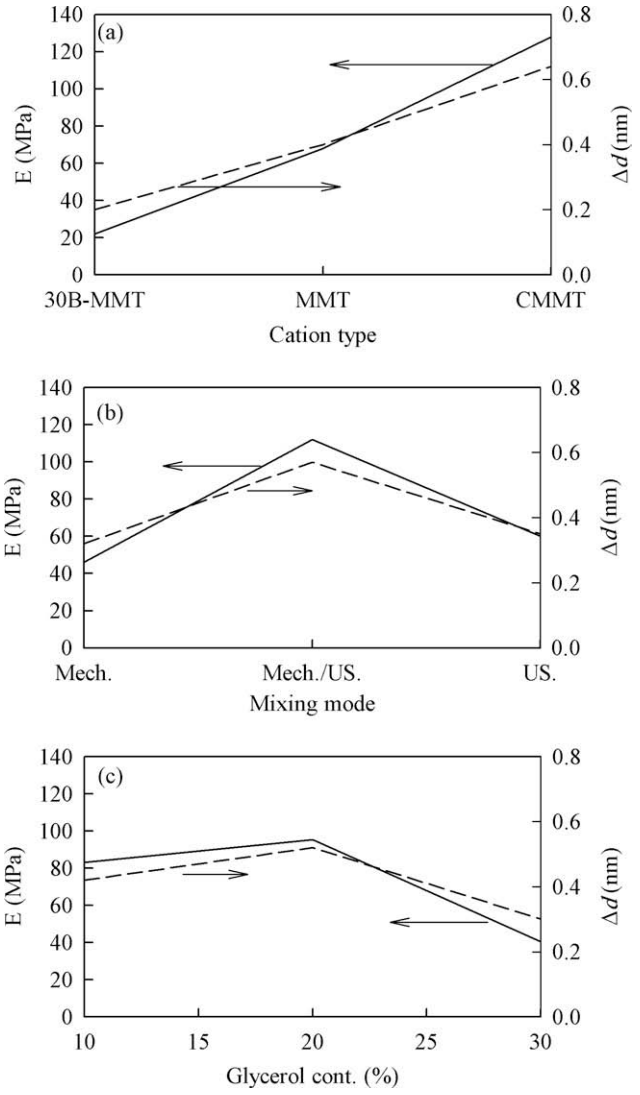

Fig. 3. Effect of factors: (a) clay cation, (b) mixing mode, (c) glycerol content on Δd and Young's modulus of nanocomposites with 5% clay.

alternating high-pressure and low-pressure cycles. This in turn subjects mechanical stress on the aggregated particles. During the low-pressure cycle, some small bubbles are created in the liquid, as the liquid vapor pressure is attained. When the bubbles reach a certain size, they collapse violently during a high-pressure cycle. This is the cavitation process that occurs near the solid surfaces. Collapsing the bubbles in affinity of solid particles leads to drives high-speed jets of liquid into the surface. These jets make ultrasound, an effective means for the breaking of agglomerates and dispersing of clay particles throughout the matrix (Doctycz & Suslick, 1990; Suslick & Grinstaff, 1991; Suslick et al., 1999).

3.4.3. Effect of glycerol content

The effect of glycerol content on the responses is shown in Fig. 3c. It can be seen that Δd and E have the highest value when 20% glycerol is used during the nanocomposite preparation. The lower or higher levels of glycerol content do not result in proper gallery spacing and therefore Young's modulus. Similar behaviors were found by Chiou et al. (2007), who compared the effects of 5%, 10%, and 15% by weight of glycerol on clay dispersion in extruded starch/clay nanocomposites. In that work, the addition of 5 wt.% glycerol has led to an exfoliated structure, whereas with 10% or 15% glycerol the intercalated morphologies have been obtained. It is implied that the sufficient amounts of glycerol plasticize the starch matrix and improves the intercalation process. However, incorporating an extra amount of glycerol into the starch/clay samples inhibits the intercalation of starch into the galleries. This is because the excess amount of glycerol leads to an increase in glycerol–starch interactions that might compete with interactions between glycerol, starch, and the clay surface.

3.4.4. Effect of starch source

As it is observed in ANOVA table, the starch source is the only factor that in the range of the examined levels does not affect the *d*-spacing and mechanical properties of nanocomposite samples. Actually, it is the amylose to amylopectin ratio in the conventional sources of starch that may differ in some degrees, and that can not affect anyway the final properties of nanocomposites most probably due to similarity in the functional groups of these two structures.

3.4.5. Optimum conditions

The optimum conditions to attain a starch/clay nanocomposite with maximum tensile properties can be determined from maximum points in main-effect plots (Fig. 4a–c). The nanocomposite with optimum properties is therefore obtained when CMMT (mixed with water by combination of mechanical mixing and ultrasonic) is used with 20% by weight of glycerol. Since the starch source was found to be insignificant factor, the economical level (potato starch, for example) can be chosen for this factor in order to decrease the costs.

Applying the optimum condition, the contribution of each factor on improvement of response can be found using Taguchi approach (Roy, 2001):

- Starch source (A): 9.90 MPa,
- Clay cation (B): 55.13 MPa,
- Glycerol content (C): 22.35 MPa,
- Mixing mode (D): 39.41 MPa.

The expected result (Young's modulus) at optimum condition is therefore predicted to be about 200 MPa.

3.5. Effect of clay content on mechanical properties

The tensile tests were performed on the prepared nanocomposite films at optimum condition with 0, 3, 4, 5, 6, 7, 10 and 15 wt.% of CMMT. Fig. 4 shows the stress–strain curves for the nanocomposite samples. It is observed that the maximum stress strength, the stress at break and Young's modulus improve with the clay content up to 6%. The tensile strength of packaging film must be more than 3.5 MPa, according to conventional standards (Kim,

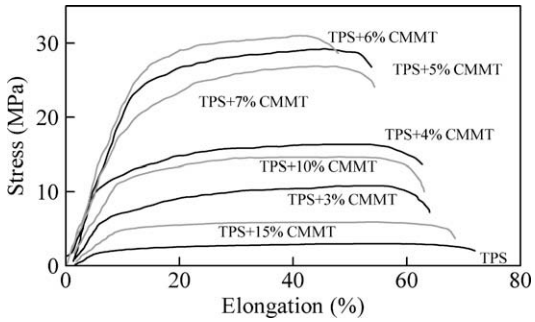

Fig. 4. The stress–strain curves of TPS and CMMT nanocomposites with different clay contents.

Lee, & Park, 1995). Thus, the value of over 30 MPa for TPS/CMMT (6%) sample is a superior value for its use as a disposable packaging film.

A higher loading however has a deterioration effect. Indeed, the improvement is usually continued with increasing the clay content up to a percent at which the silicate layers cannot be exfoliated anymore. Afterwards, addition of more amount of clay into the matrix leads to appearance of clay stacks and even aggregates that deteriorate the mechanical properties.

In the case of elongation at break, the addition of clay content first results in a reduction in this property, up to 6% clay content. This can be attributed to the fact that the layered silicates might provide some new nucleation sites and thus contribute in growth of crystallites (Cyras et al., 2008). The crystallization process causes the brittleness of nanocomposites and reduces their strain at break (Magalhaes & Andrade, 2009). Addition of more amounts of nanoclays however, causes an adverse effect so that the elongation at break is increased. The strong interaction of starch molecules with water (through ion–dipole interactions) may help retain moisture in the samples that leads to a plasticizing effect and therefore a greater elongation at break (Dean et al., 2007). These two phenomena lead to a minimum value for elongation at break in nanocomposites with 6 wt.% clay.

3.6. FT-IR analysis

The FT-IR spectra of CMMT, pristine starch, TPS and nanocomposite containing 6 wt.% CMMT are shown in Fig. 5. The minor shifts in characteristic peaks of the TPS and nanocomposite spectra with respect to that of pristine starch could probably reveal the formation of secondary interactions in the TPS and nanocomposite as proposed also by the other authors (Huang, Yu, & Ma, 2005; Ning, Xingxiang, Na, & Shihe, 2009; Zhang, Chang, Wu, Yu, & Ma, 2008). Based on the harmonic oscillator mode for analysis of vibration of chemical bonds, the reduction in force constant Δf could be represented by following equation:

$$\Delta f = f_p - f_{np} = \frac{\mu(v_p^2 - v_{np}^2)}{4\pi^2} \quad (1)$$

where $\mu = m_1 m_2/(m_1 + m_2)$ corresponds to the reduced mass of the oscillators; v, is the oscillating frequency, and f is the force constant. The subscripts np and p denote non-plasticized and plasticized oscillators, respectively. The reduction of force constant brought about by some interaction formed between polymer and plasticizer is directly related to the frequency (or wave number) shift of stretching vibrations because of the reduction of bond forces. Thus, the lower the peak frequency in FT-IR spectra of TPS or nanocomposite compared with that in virgin starch, the stronger is the new interaction with respect to previous one (Pawlak & Mucha, 2003).

As shown in Fig. 5, generally the characteristic peaks were appeared at lower wave numbers in TPS than those in neat starch. On the other hand, the presence of glycerol could decrease the wave number of the peak, ascribed to C–O stretch of C–O–H in starch at 1156 and 1081 cm^{-1} and C–O stretch of C–O–C in starch at 1020 cm^{-1}. This is due to the fact that plasticizer could form intense H-bonding interaction with the hydroxyl groups of starch molecules, and thus displaces the peaks. Compared with TPS, some of these characteristic peaks in TPS/CMMT nanocomposites are in turn situated at the lowest wave numbers, most probably owing to the strong interactions of starch–citric acid in this nanocomposite. As discussed before, the citric acid molecules play a roll of bridge between clay surface and starch molecules through hydrogen bonding. This leads to higher performance of intercalation process in corresponding nanocomposites. Moreover, these shifts are

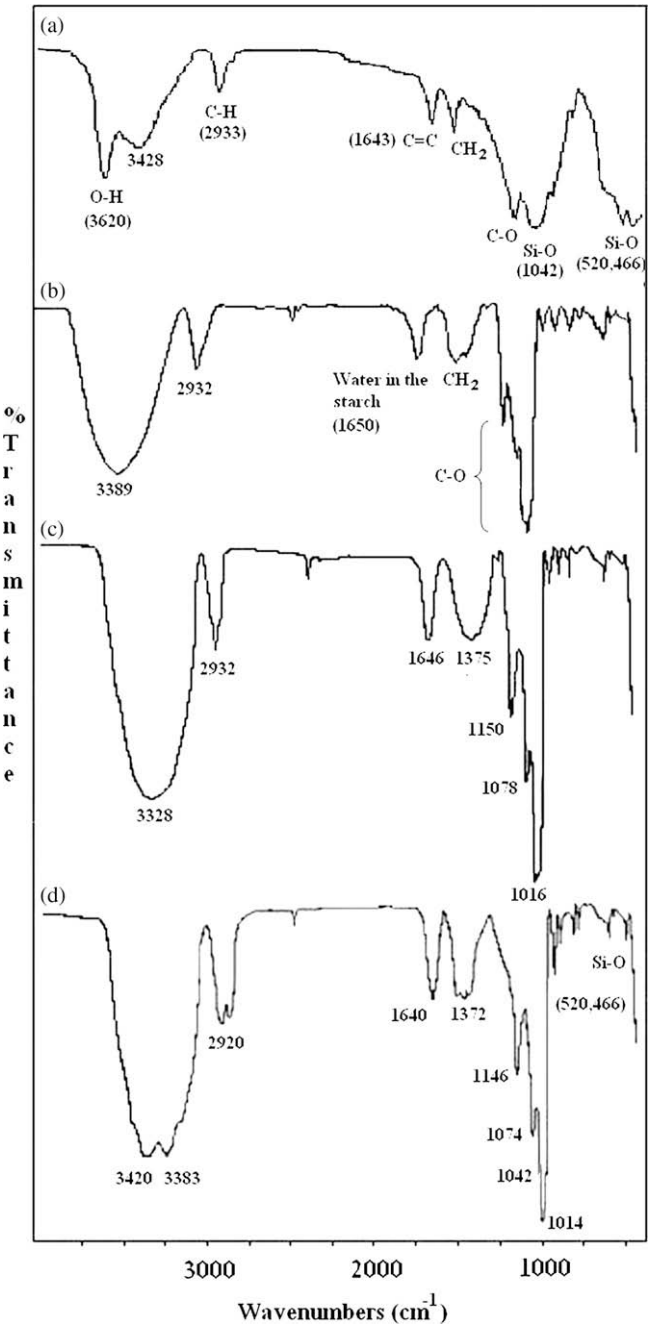

Fig. 5. FT-IR spectra of (a) CMMT, (b) starch, (c) TPS, and (d) TPS/CMMT nanocomposite (6 wt.%).

the representatives of fragmentation and dissolution of starch granules by citric acid (Ning et al., 2009). Actually, the destroyed starch structure can be permeated by plasticizer easily that paves the way for citric acid to increase the interaction between starch and glycerol in these nanocomposites (Wang, Yu, & Han, 2007). The original hydroxyl interactions in starch are therefore weakened by the formation of new more stable hydrogen bonds between starch, glycerol and citric acid. This in turn moves slightly the absorbance frequency in FT-IR spectra of hydroxyl group in TPS/CMMT nanocomposite to lower values. It is implied that the C–H bond in stretch mode for CH_2 in glucose ring (2932 cm^{-1}) has not been taken part in the formation of hydrogen bonds in the starch plasticization process, so its oscillation frequency has not been changed.

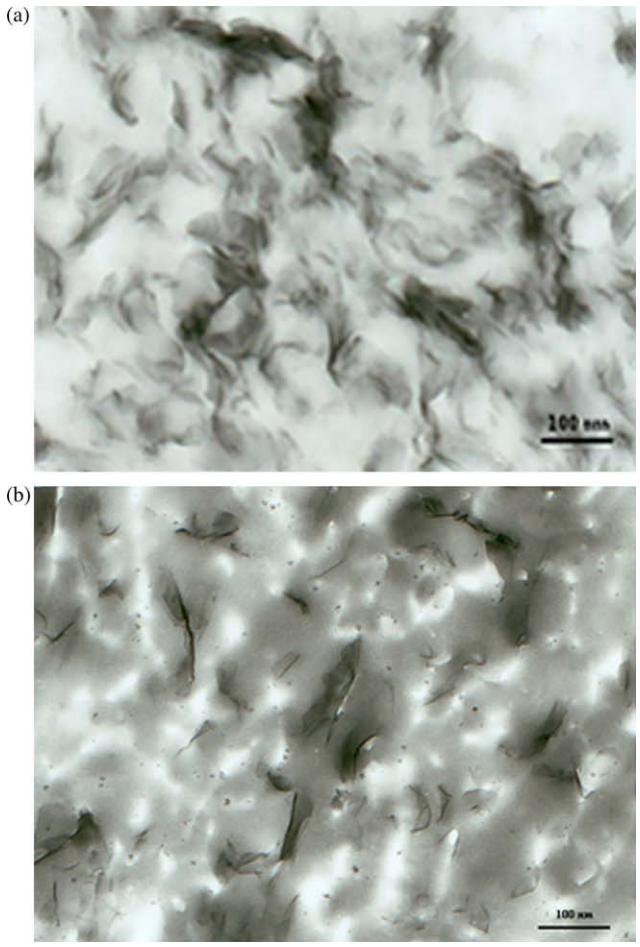

Fig. 6. TEM micrographs of TPS/CMMT nanocomposites with (a) 6 wt.% CMMT, and (b) 10 wt.% CMMT.

3.7. Morphology

The TEM micrographs of two nanocomposite samples with different loadings of CMMT are shown in Fig. 6. In nanocomposite with 6 wt.% of CMMT (Fig. 6a) the clay particles are well dispersed throughout the polymer matrix so that an intercalative/exfoliated structure is obtained. As the clay content is increased to 10 wt.%, some agglomerations of platelets are observed (Fig. 6b). These two micrographs justify well the mechanical behaviors of nanocomposite films as shown in Fig. 4. In the former, the silicate layers are expanded and evenly dispersed in the TPS phase in nanometer sizes so that they can play the role of reinforcing action into the matrix. Increasing the clay content however, may lead to formation of agglomerates, as illustrated for 10 wt.% samples.

4. Conclusions

Plasticized starch/clay nanocomposites were prepared by solution casting technique and the influences of various factors on the morphology and mechanical properties (tensile strength and Young's modulus) of these nanocomposites were statistically analyzed using Taguchi experimental approach. The main conclusions in the range of considered levels can be listed as follow:

- The mechanical properties are strongly influenced by the clay cation type, the clay mixing mode, and the glycerol content, respectively. The starch source namely the amylase to amylopectin ratio was found to be an insignificant factor in this study.
- The clay modified by citric acid (CMMT), represented better mechanical properties in comparison with MMT and 30B–MMT. The interactions between citric acid and starch chains were responsible for this improvement.
- Nanocomposite samples prepared with combination of mechanical and ultrasonic mixing modes represented the best dispersion degree of silicate layers compared to either mechanical or ultrasonic due to contribution of both dispersive and distributive mixing mechanisms.
- The optimum conditions for preparation of starch/clay nanocomposites were obtained as follow: Potato starch, CMMT clay, 20% glycerol and combined mechanical/ultrasonic mixing modes.
- The tensile strength and Young's modulus of the nanocomposite samples were best improved with 6 wt.% of CMMT due to its intercalated/exfoliated morphology.

Acknowledgement

This work was financially supported, in part, by the Iranian Nanotechnology Initiative.

References

Avella, M., De Vlieger, J. J., Errico, M. E., Fischer, S., Vacca, P., & Volpe, M. G. (2005). Biodegradable starch/clay nanocomposite films for food packaging applications. *Food Chemistry, 93*, 467–474.

Chen, B., & Evans, J. R. G. (2005). Thermoplastic starch–clay nanocomposites and their characteristics. *Carbohydrate Polymers, 61*, 455–463.

Chiou, B., Wood, D., Yee, E., Imam, S. H., Glenn, G. M., & Orts, W. J. (2007). Extruded starch–nanoclay nanocomposites: Effects of glycerol and nanoclay concentration. *Polymer Engineering and Science, 47*, 1898–1904.

Chiou, B. S., Yee, E., Glenn, G. M., & Orts, W. J. (2005). Rheology of starch–clay nanocomposites. *Carbohydrate Polymers, 59*, 467–475.

Curvelo, A. A. S., Carvalho, A. J. F., & Agnelli, J. A. M. (2001). Thermoplastic starch–cellulosic fibers composites: Preliminary results. *Carbohydrate Polymers, 45*, 183–188.

Cyras, V. P., Manfredi, L. B., Ton-That, M. T., & Vazquez, A. (2008). Physical and mechanical properties of thermoplastic starch/montmorillonite nanocomposite films. *Carbohydrate Polymers, 73*, 55–63.

Dean, K., Yu, L., & Wu, D. Y. (2007). Preparation and characterization of melt-extruded thermoplastic starch/clay nanocomposites. *Composites Science and Technology, 67*, 413–421.

Doctycz, S. J., & Suslick, K. S. (1990). Interparticle collisions driven by ultrasound. *Science, 247*, 1067–1069.

Hasebawa, N., Kawasumi, M., Kato, M., Usuki, A., & Okada, A. (1998). Preparation and mechanical properties of polypropylene–clay hybrids using a maleic anhydride-modified polypropylene oligomer. *Journal of Applied Polymer Science, 67*, 87–92.

Huang, M., Yu, J., & Ma, X. (2005). Ethanolamine as a novel plasticiser for thermoplastic starch. *Polymer Degradation and Stability, 90*, 501–507.

Huang, M., Yu, J., & Ma, X. (2006). High mechanical performance MMT–urea and formamide-plasticized thermoplastic cornstarch biodegradable nanocomposites. *Carbohydrate Polymers, 63*, 393–399.

Kampeerapappun, P., Aht-ong, D., Pentrakoon, D., & Srikulkit, K. (2007). Preparation of cassava starch/montmorillonite composite film. *Carbohydrate Polymers, 67*, 155–163.

Kim, Y. J., Lee, H. M., & Park, O. O. (1995). Processabilities and mechanical properties of Surlyn-treated starch/LDPE blends. *Polymer Engineering and Science, 35*, 1652–1657.

Magalhaes, N. F., & Andrade, C. T. (2009). Thermoplastic corn starch/clay hybrids: Effect of clay type and content on physical properties. *Carbohydrate Polymers, 75*, 712–718.

Mondragon, M., Mancilla, J. E., & Rodriguez-Gonzalez, F. J. (2008). Nanocomposites from plasticized high-amylopectin, normal and high-amylose maize starches. *Polymer Engineering and Science, 48*, 1261–1267.

Montgomery, D. C. (1997). *Design and analysis of experiments*. New York: John Wiley & Sons.

Ning, W., Xingxiang, Z., Na, H., & Shihe, B. (2009). Effect of citric acid and processing on the performance of thermoplastic starch/montmorillonite nanocomposites. *Carbohydrate Polymers, 76*, 68–73.

Pandey, J. K., & Singh, R. P. (2005). Green nanocomposites from renewable resources: Effect of plasticizer on the structure and material properties of clay-filled starch. *Starch, 57*, 8–15.

Park, S. H. (1996). *Robust design and analysis for quality engineering*. London: Chapman & Hall.

Park, H. M., Lee, W. K., Park, C. Y., Cho, W. J., & Ha, C. S. (2003). Environmentally friendly polymer hybrids. *Journal of Materials Science, 38*, 909–915.

Paul, E. L., Atiemo-Obeng, V. A., & Kresta, S. M. (2004). *Handbook of industrial mixing*. New Jersey: John Wiley & Sons.

Pawlak, A., & Mucha, M. (2003). Thermogravimetric and FT-IR studies of chitosan blends. *Thermochimica Acta, 396*, 153–166.

Ray, S. S., & Bousmina, M. (2005). Biodegradable polymers and their layered silicate nanocomposites: In greening the 21st century materials world. *Progress in Materials Science, 50*, 962–1079.

Roy, K. R. (2001). *Design of experiments using Taguchi approach: 16 steps to product and process improvement*. New York: John Wiley & Sons.

Sorrentino, A., Gorrasi, G., & Vittoria, V. (2007). Potential perspectives of bio-nanocomposites for food packaging applications. *Trends in Food Science and Technology, 18*, 84–95.

Suslick, K. S., Didenko, Y., Fang, M. M., Hyeon, T., Kolbeck, K. J., McNamara, W. B., et al. (1999). Acoustic cavitation and its chemical consequences. *Philosophical Transactions of the Royal Society Series A, 357*, 335–353.

Suslick, K. S., & Grinstaff, M. W. (1991). Proteinaceous microbubbles: Synthesis of an echo contrast agent. *Proceedings of the National Academy of Sciences of the United States of America, 88*, 7708–7710.

Tang, X. (2008). Use of extrusion for synthesis of starch–clay nanocomposites for biodegradable packaging films. PhD. Thesis, Kansas State University.

Wang, N., Yu, J. G., & Han, C. M. (2007). Influence of citric acid on the properties of glycerol-plasticised cornstarch extrusion blends. *Polymers & Polymer Composites, 15*, 545–552.

Wilhelm, H. M., Sierakowski, M. R., Souza, G. P., & Wypych, F. (2003). Starch films reinforced with mineral clay. *Carbohydrate Polymers, 52*, 101–110.

Yaws, C. L. (1999). *Chemical properties handbook*. New York: McGraw Hill.

Yu, J., Wang, J., Wu, X., & Zhu, P. (2008). Effect of glycerol on water vapor sorption and mechanical properties of starch/clay composite films. *Starch, 60*, 257–262.

Zhang, J., Chang, P. R., Wu, Y., Yu, J., & Ma, X. (2008). Aliphatic amidediol and glycerol as a mixed plasticizer for the preparation of thermoplastic starch. *Starch, 60*, 617–623.